Momentum-shell renormalization-group flow from simulation

A. Tröster*
Faculty of Physics, University of Vienna, Boltzmanngasse 5, A-1090 Vienna, Austria
(Received 31 October 2008; published 26 March 2009)

Our recently developed Fourier Monte Carlo algorithm permits a nonperturbative calculation of momentum-shell renormalization-group flows by simulation which despite its apparent simplicity is illustrative both numerically as well as conceptually interesting. We study the example of a ϕ^4 model with long-range lattice interaction. For this model we show that the topology of the renormalization flow is globally accessible in a particularly convenient way. The nontrivial fixed point of Wilson-Fisher type is observed its accompanying critical exponents are numerically determined from fitting its surrounding flow pattern to a linearized renormalization-group transformation. The results are compared to those obtained from perturbation theory, ϵ-expansion and earlier Monte Carlo simulations. Application of our method is also expected to be rewarding in other models with long-range interactions.

DOI: 10.1103/PhysRevE.79.036707 PACS number(s): 05.10.Ln, 05.10.Cc

The paradigm of the renormalization group (RG) continues to represent a major line of thinking in modern theoretical physics. Resembling a milestone in our understanding of the physics of collective behavior of a large number of degrees of freedom, RG ideas are of central importance in such diverse fields as the theory of phase transitions and quantum field theory [1,2], strongly correlated quantum systems [3], or turbulence [4]. Resting on such fundamental concepts such as scale invariance, asymptotic behavior, power laws, and self-similarity, it is not surprising that the rather abstract underlying philosophy of the RG also manifest itself in a large diversity of different computational schemes. However, momentum shell renormalization-group transformations in combination with the ϵ-expansion [5,6] are usually the method of choice employed in the literature [7] when it comes to introducing RG fundamentals, as it neither requires complicated mathematics nor abstract field theoretic concepts. The general strategy consists of constructing a recursion relation for the effective Hamiltonian of "slow" (i.e., long wavelength) degrees of freedom of a given system by integrating over the "fast" variables residing in a wave vector "shell" $\Lambda/b<|\boldsymbol{k}|<\Lambda$, $b>1$, below [8] a given wave-vector cutoff Λ. This coarse-graining (CG) step is followed by accompanying rescaling operations to restore the original cutoff Λ, which must be tuned in a delicate way to allow for a nontrivial fixed point (FP). In analyzing the topology of the resulting flow in the space of coupling constants, the notion of relevant, irrelevant, and marginal couplings and the concept of universality naturally emerges. Once the FP is known, the critical exponents can in principle be calculated from the fixed rescaling factor and the eigenvalues of the linearized RG transform at this FP.

All of the above reasoning is in principle exact. Analytically, however, the CG step is difficult to carry out, and one needs to resort to approximative methods. Unfortunately, a perturbative treatment seemed to lack a corresponding "small parameter." However, analyzing the archetypical case of the so-called Landau-Ginzburg (LG) or ϕ^4 model with dimensionless Hamiltonian $\mathcal{H}[s]=\int d^dx[\frac{K_2}{2}(\nabla s)^2(\boldsymbol{x})+\frac{r_0}{2}s^2(\boldsymbol{x})+\frac{u_0}{4}s^4(\boldsymbol{x})]$ with short-range (SR) lattice interaction $\int_{\boldsymbol{x}}\frac{K_2}{2}(\nabla s)^2(\boldsymbol{x})$, Wilson and Fisher [5] observed that while above the critical dimension $d_c^{(\mathrm{SR})}=4$ the physical critical behavior is governed by the Gaussian fixed point values $(u_0^*,r_0^*)=(0,0)$, for $d<d_c^{(\mathrm{SR})}$ the fixed point couplings u_0^* and r_0^* are both proportional to $\epsilon=4-d$, which can therefore serve as the sought-after expansion parameter. Unfortunately, within Wilson's original momentum-shell scheme, concrete perturbative corrections beyond $O(\epsilon^2)$ turn out to be of formidable complexity. Instead, in a number of important cases, field theoretic perturbation theory augmented by sophisticated Borel or variational resummation techniques [9] provides a practical calculation scheme to compute universal quantities with high precision.

After several decades of research, however, it is sobering to find that fortunate properties like Borel summability of the resulting asymptotic series is rather the exception than the rule and has only been proven in rare instances, Also, frequently the required information on higher perturbative orders is simply not available [1]. Therefore, nonperturbative approaches are at the present focus of attention [2]. Analytically, this represents a formidable challenge. Nevertheless, it is clear that computer simulations, in particular of the Monte Carlo (MC) type, in particular if combined with finite-size scaling, are capable of yielding "exact" results. However, for a number of reasons it seems difficult to combine a MC type of approach with Wilson's original momentum-shell prescription. First, quite trivially, simulations are confined to systems of integer dimension d, such that the gradual separation of the Wilson-Fisher fixed point (WFFP) (u_0^*,r_0^*) from the Gaussian fixed point (0, 0) for growing ϵ cannot be studied systematically. Also, instead of momentum space, conventional MC simulations are set up on direct space lattices, for which Wilson's momentum space coarse-graining step is extremely cumbersome to reproduce. As we have recently shown [10], the latter difficulty can, however, be avoided by performing MC simulations directly in Fourier space, using the real and imaginary parts of the order parameter Fourier amplitudes as basic MC variables. We refer to Ref. [10] for a detailed description of this algorithm. Within the standard

*andreas.troester@univie.ac.at

short-range LG model, however, also our Fourier Monte Carlo (FMC) based approach faces considerable difficulties. Again, only d=integer is possible. According to an ϵ-expansion analysis, in $d=4$ the Gaussian fixed point (GFP) and the WFFP coincide, while in $d=3$ dimensional analysis suggests that in principle at least a sixth-order interaction $(u_0/6)s^6(\boldsymbol{x})$ should also be kept in the Hamiltonian, which considerably diminishes the efficiency of the algorithm presented in Ref. [10]. Moreover, in order to reach the WFFP, it is necessary to determine the field rescaling factor $z(b)=b^{(d+2-\eta_{\mathrm{SR}})/2}$, i.e., the exponent η_{SR}, from the requirement to keep the rescaled coefficient K_2 of the transformed gradient dispersion term $K_2(\nabla s')^2(\boldsymbol{x})$ unchanged. While in a real space simulation we are not aware of any straightforward way to achieve this, in FMC the CG dispersion can indeed been determined [10] and—outside the critical region—was observed to be rather inert. Inside the critical region, we therefore suspect that (owing to the actual smallness of the exponent η) extensive numerical work may be required to compute $z(b)$ with sufficient precision.

Fortunately, there is a model closely related to the original LG model, which allows us to overcome most of the above difficulties. In this model, the SR lattice interaction is complemented by an additional long-range (LR) interaction of type $\int d^dx \int d^dy (K_\sigma/2)\frac{s(\boldsymbol{x})s(\boldsymbol{y})}{|\boldsymbol{x}-\boldsymbol{y}|^{d+\sigma}}$, where $\sigma>0$ ensures existence of the thermodynamic limit. In momentum space, this leads to an additional "σ-dispersion" $(1/2)K_\sigma|\boldsymbol{k}|^\sigma$ apart from the analytic gradient term $(1/2)K_2|\boldsymbol{k}|^2$. A RG analysis of this model [11–15] shows that for $\sigma>2$, this term is irrelevant and the critical behavior of the model is that of the LG universality class. However, for $\sigma<2$ the long-range character of the interaction becomes effective. By definition, above the σ-dependent upper critical dimension $d_c^{(\mathrm{LR})}(\sigma)=2\sigma$, the model appears to follow mean-field behavior, while for $d<d_c^{(\mathrm{LR})}(\sigma)$ a long-range fixed point (LRFP) similar to the WFFP appears that governs the critical behavior. Since the "small" perturbative expansion parameter is now $\tilde{\epsilon}:=d_c(\sigma)-d=2\sigma-d$, the fact that $d_c^{(\mathrm{LR})}(\sigma)$ can be "tuned" with σ allows for the $\tilde{\epsilon}$-expansion to be reinterpreted [11] as an expansion for fixed d and variable σ. As the corresponding corrections are purely analytic, the requirement of K_σ to be invariant yields $z(b)=b^{(d+\sigma)/2}$ and thus $\eta_{\mathrm{LR}}=2-\sigma$ to all orders of perturbation theory, a RG result which has also been confirmed numerically [14,15]. From the point of view of simulations, this is a large technical advantage over the SR case: Here we do not have to determine $z(b)$ or η from fitting dispersion corrections—*they are known exactly*. Since an arbitrary coupling term in the Hamiltonian involving q spatial derivatives and $2n$ powers of $s(\boldsymbol{x})$ is found to receive a rescaling factor $b^{n\sigma-(1-n)d-q}$, actually only r_0, u_0, and K_2 remain on the list of "interesting" couplings. Among these, the "temperature" r_0 corresponds roughly to the single relevant direction in parameter space, as necessary for a generic critical point in the absence of an external field. Short-range lattice interactions are always present in a real system, but the overall scaling factor $b^{\sigma-2}$ signals the irrelevance of K_2 in this RG transformation. Nevertheless, even if initially $K_2=0$, coarse graining will produce a nonzero coefficient representing the analytic dispersion flow. In fact, Sak [13] argues that the crossover to the short-range LG model takes place not at $\sigma=2$ but already at $\sigma=2-\eta_{\mathrm{SR}}$, removing a superficial jump discontinuity of η_{LR} as $\sigma\to 2$. This odd behavior is attributed to the increasingly non-negligible effect of the flow around the fixed point value K_2^*, which is only zero to order $\tilde{\epsilon}$. In fact this point is still under considerable debate (cf. the discussion in Ref. [15]). At present we only point out that the SR coupling term must be properly taken into account when attempting to study this crossover behavior. Summarizing the situation, at fixed $d=3$ and $1.5\leqslant\sigma\ll 2-\eta_{\mathrm{SR}}\approx 1.97$ we should get away with studying the projection of the corresponding SRFP and their global surrounding RG flow onto the (u_0,r_0) plane.

Our simulations are built on a simple three-dimensional (3D) cubic lattice with $N=L^3$ sites, lattice constant $a=1$, and periodic boundary conditions. To avoid finite-size inaccuracies in the definition of the spatial scaling parameter b, we introduce cubic (instead of spherical) cutoffs $\Lambda=2\pi l/L$, $\Lambda'=2\pi l'/L 1\leqslant l'<l\leqslant L/2$ parametrized by integers l,l' for the wave-vector components $k_i=2\pi m_i/L$, $-L/2+1\leqslant m_i\leqslant L/2$, $m_i\in\mathbb{Z}$ and set $b\equiv l/l'$, such that $\Lambda'=\Lambda/b$. The corresponding coarse-grained coefficients $\tilde{u}_0=\tilde{u}_0(u_0,r_0,\Lambda,b)$, $\tilde{r}_0=\tilde{r}_0(u_0,r_0,\Lambda,b)$ are obtained from a polynomial fit [10] of the effective free energy as a function of $\tilde{s}(\boldsymbol{0})$ by averaging out all Fourier amplitudes $\tilde{s}(\boldsymbol{k})$ for $\Lambda/b<|\boldsymbol{k}_i|\leqslant\Lambda$. To determine the central barrier and the "wings" of this free energy accurately, we combine the Wang-Landau approach [16] with our FMC algorithm. We also need to address the question of how to find a lattice-periodic dispersion resembling $|\boldsymbol{k}|^\sigma$. As a nearest-neighbor interaction translates into a lattice dispersion $4\Sigma_{i=1}^d \sin^2\frac{k_i}{2}$, we replace the continuum long-range dispersion $|\boldsymbol{k}|^\sigma$ by $\omega^\sigma(\boldsymbol{k};1)$, where we abbreviate $\omega^2(\boldsymbol{k};n):=\Sigma_{i=1}^d(4\sin^2\frac{k_2}{2})^n$. To shift the cubic anisotropy in this expression further towards the Brillouin zone boundary, we actually used the slightly "improved" long-range dispersion form

$$|\boldsymbol{k}|^\sigma := \omega^2(\boldsymbol{k};1)\left(1+\frac{\sigma}{24}\frac{\omega^2(\boldsymbol{k};2)}{\omega^2(\boldsymbol{k};1)}\right). \tag{1}$$

A total of 30×30 initial parameter points (u_0,r_0) was used to determine each RG flow, and each such flow diagram was averaged over 10 independent sets, yielding a total of 9000 individual Wang-Landau simulations per diagram. To locate the WFFP $\boldsymbol{K}^*\equiv(u_0^*,r_0^*)$ and determine the critical exponents governed by the flow $\boldsymbol{K}=(u_0,r_0)\to\boldsymbol{K}'=(u_0',r_0')$, we again proceed in the spirit of the RG. In the vicinity of $\boldsymbol{K}^*$ the flow is approximated by a linearized RG of type

$$\boldsymbol{K}'=\boldsymbol{K}^*+\boldsymbol{R}\cdot(\boldsymbol{K}-\boldsymbol{K}^*). \tag{2}$$

The exact location $\boldsymbol{K}^*$ and the matrix elements $R_{ij},i,i=1,2$ can thus be determined from a least-squares fit of this equation in the approximate neighborhood of the fixed point. From the eigenvalues λ_τ and λ_u of $\boldsymbol{R}$ we estimate the correlation length exponent $\nu=1/y_\tau$ and the leading irrelevant exponent $\omega=-y_u$, where $y_i=\ln\lambda_i/\ln b$, $i=\tau,u$. In Fig. 1, we show a prototypical fit obtained for the RG flow at $L=36$, $\sigma=1.65$, $K_2=0$, and $K_\sigma=1$, subject to cutoffs parametrized by $l=9$, $l'=7$, i.e., $b=9/7$. Such simulations were performed for several values of σ in the region $0.58\leqslant\sigma\leqslant 0.7$. For

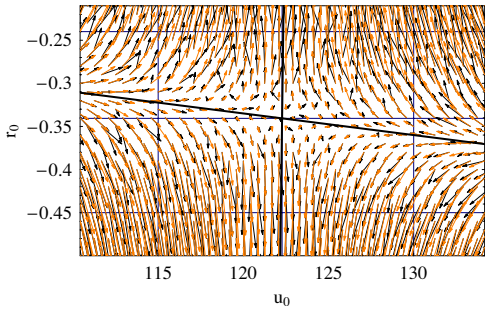

FIG. 1. (Color online) RG flow in the (u_0, r_0) plane around the SRFP. Parameters $L=36$, $\sigma=1.65$, $l=9$, $b=9/7$. Black, simulation results; orange (gray), fit to linearized RG transformation (fit region indicated). The two thick black lines denote the eigendirections of the linearized transformation.

smaller σ, i.e., in the crossover region $1.5<\sigma<0.58$ to the Gaussian fixed point we were unable to locate $\boldsymbol{K}^*$ with sufficient accuracy.

In principle, the results for the location of the nontrivial fixed point and the exponent y_τ obtained by the method sketched above can be compared to the corresponding analytical $\tilde{\epsilon}$-expansion predictions. However, when attempting such a comparison, one should be aware of several sources of discrepancy, which will generally affect the numerical values of both nonuniversal as well as universal quantities.

As to the nonuniversal ones, in fitting the RG flow to the linearized ansatz (2), the choice of the fitting range surrounding the RGFP has a tiny but non-negligible effect on the results due to flow nonlinearities. More interestingly, it is clear that simulations of the above type must necessarily be performed on finite systems and are therefore contaminated by a certain finite-size effect. Somehow related to this problem is the fact that to compute the RG flow the coarse-graining step of the RG transformation must be carried out using a momentum shell of finite thickness instead of the infinitesimally thin one (setting $b=1+\delta$, $\delta\to 0$) that is used in analytical calculations at the thermodynamic limit. Apart from this, it is well known that, as a rule, the location of $\boldsymbol{K}^*$ itself, which is calculated as

$$u_0^* = \frac{\pi^\sigma \Gamma(\sigma)}{9\times 2^{1-2\sigma}}\tilde{\epsilon} + O(\tilde{\epsilon}^2), \tag{3}$$

$$r_0^* = -\frac{\Lambda^\sigma}{3\sigma}\tilde{\epsilon} + O(\tilde{\epsilon}^2) \tag{4}$$

for $d=3$ and $K_\sigma=1$, cannot be expected to be universal anyway, as, e.g., r_0 depends manifestly on the cutoff Λ. In addition, the cutoff geometry is chosen to be spherical in the analytic calculation, while a cubic one is used in the simulation. On the other hand, the analytic values (3) and (4) only represent perturbative first-order results in $\tilde{\epsilon}$.

We now turn to the discussion of the numerical values found for the universal quantities. As to the analytical calculation of critical exponents, the result for the exponent γ in order $\tilde{\epsilon}^2$ was announced in Ref. [11], and the "sticking" of η to the value $\eta=2-\sigma+O(\tilde{\epsilon}^3)$ was verified to third order. From these expressions, all other (leading) exponents can thus be calculated in order $\tilde{\epsilon}^2$ by employing the usual scaling relations. Here we quote the result announced for the exponent y_τ as [14]

$$y_\tau = \sigma - \frac{\tilde{\epsilon}}{3} - \frac{1}{6}\frac{\mathcal{A}(\sigma)}{\sigma}\tilde{\epsilon}^2 + O(\tilde{\epsilon}^3), \tag{5}$$

where, denoting the digamma function by $\psi(z) := \Gamma'(z)/\Gamma(z)$, we abbreviate

$$\frac{\mathcal{A}(\sigma)}{\sigma} = \psi(1) - 2\psi(\sigma/2) + \psi(\sigma). \tag{6}$$

Unfortunately, details of the derivation of these formulas, which were carried out using the "matching condition technique" of Wilson [17] instead of an even more laborious second-order momentum-shell calculation, seem to have never been presented, but the calculations are reported to be quite involved [11]. As to the $\tilde{\epsilon}$-expansion calculation of the first subleading correction exponent ω, we are only aware of the first-order result

$$\omega = 2\sigma - 3 + O(\tilde{\epsilon}^2). \tag{7}$$

In any case, we should be prepared to observe that as far as the values obtained for the critical exponents from our simulations are concerned, the results will only be of an accuracy similar to those of the first-order $\tilde{\epsilon}$-expansion. This is a simple consequence of the fact that even though a MC simulation is "nonperturbative" in nature, in evaluating the resulting data the full RG flow is projected onto the two-dimensional (u_0, r_0) plane, not taking into account the flow in the remaining directions in the full (infinite-dimensional) space of coupling constants, which is very much in the spirit of the $\tilde{\epsilon}$-expansion. In addition, the finite system size will also introduce a corresponding error in determining the critical exponents.

Despite the above difficulties, it is interesting to compare our present simulations to results obtained from a first-order perturbative approach. In the thermodynamic limit, the corresponding Feynman diagrams would be calculated as momentum-shell integrals. To permit a "fair" comparison to our results, which are calculated for a finite system, we replace these loop integrals over infinitesimally thin shells with sums over $\boldsymbol{k}$ vectors residing in the finite shell $\Lambda/b<|\boldsymbol{k}|\leqslant\Lambda$, which yields the recursion relations

$$\tilde{r}_0 = r_0 + 3u_0\frac{1}{N}\sum_{\boldsymbol{k}} \tilde{G}_{\Lambda,b}(\boldsymbol{k}), \tag{8}$$

$$\tilde{u}_0 = u_0\left(1 - 9u_0\frac{1}{N}\sum_{\boldsymbol{k}} \tilde{G}^2_{\Lambda,b}(\boldsymbol{k})\right) \tag{9}$$

valid for our finite system, where $\tilde{G}_{\Lambda,b}(\boldsymbol{k}) = 1/(|\boldsymbol{k}|^\sigma + r_0)$ for $\Lambda/b<|\boldsymbol{k}|\leqslant\Lambda$ and zero elsewhere. In this way, those discrepancies between simulation and perturbation theory which merely arise from finite-size effects and different cutoff geometries are eliminated. Indeed, at least qualitatively the global topology of the corresponding flow resembles that found in the simulations (see Fig. 2). Based on low-order perturba-

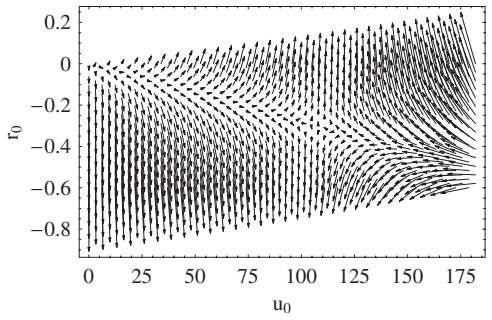

FIG. 2. Global topology of RG flow in the (u_0, r_0) plane as computed from the perturbative approximation, Eq. (9). Parameters $L=36$, $\sigma=1.65$, $l=9$, $b=9/7$.

tion theory, the locations of the corresponding calculated fixed points still show a systematic deviation from those found in the simulations. However, we are surprised to find that all fixed points obtained from simulations and perturbative calculations seem to collapse onto a single trajectory (cf. top of Fig. 3).

The subleading correction exponent ω obtained from fitting the simulated or perturbatively calculated flow patterns to a linearized RG transformation is in reasonable agreement with the corresponding $O(\tilde{\epsilon})$ results from the $\tilde{\epsilon}$-expansion (cf. Table I and the bottom figure in Fig. 3).

In contrast, for the exponent y_τ, apart from the $O(\tilde{\epsilon}^2)$ results of Eq. (5) also high-precision finite-size scaling results by Luijten [14,15] are available. Their comparison to the first-order truncated results and to those obtained from our two-dimensional flow patterns is quite instructive. As one can observe from Table I and the middle figure of Fig. 3, there is a close-to-perfect agreement of the numerical data of Refs. [14,15] with those of the second-order $\tilde{\epsilon}$-expansion predictions in the approximate range $1.5<\sigma<1.7$. The deviations observed between these high-precision studies and the second-order $\tilde{\epsilon}$-expansion result for larger values of σ should not be taken too seriously but most probably only signals the asymptotic nature of the expansion. Therefore, we are led to regarding the result of Refs. [14,15] as our basic reference result. However, in view of the above expectations on the validity of the results obtained from our restricted two-dimensional RG flow, we also find it interesting to study the first-order truncated expression $y_\tau=\sigma-\frac{\tilde{\epsilon}}{3}+O(\tilde{\epsilon}^2)$ of Eq. (5), which is seen to deviate from the second-order one rather quickly for σ increasing from $\sigma=1.5$. Indeed, it is

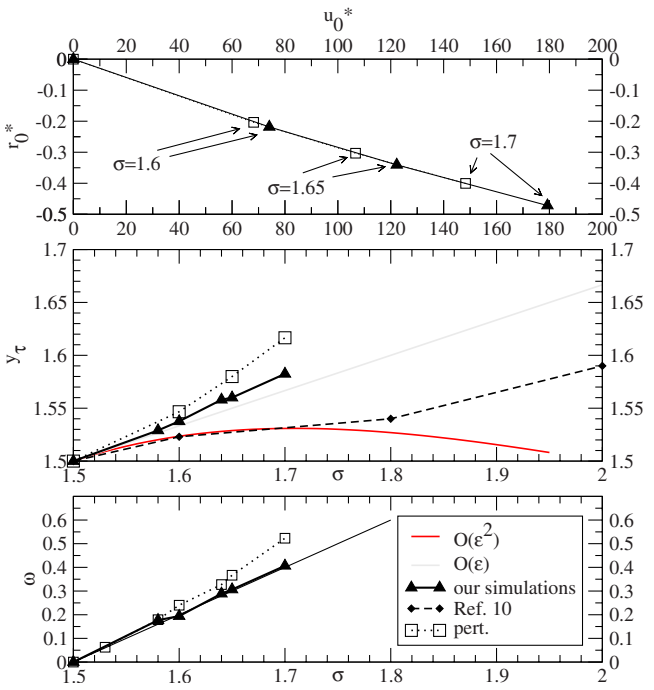

FIG. 3. (Color online) Results obtained for parameters $L=36$, $K_\sigma=1$, $l=9$, $b=9/7$. Top: Comparison of RG flow fixed point locations found from simulations and perturbation theory (lines are a guide to the eye). Middle and bottom: Exponents y_t and ω.

interesting to see that the y_τ values obtained from this first-order $\tilde{\epsilon}$-expansion turn out to be in better agreement with those calculated from our simulations than those obtained from the perturbative ones.

To obtain results valid to order $O(\tilde{\epsilon}^2)$ for the exponents from our simulations one should determine the flow pattern including the additional two dimensions represented by the leading "least-irrelevant" parameters, namely the sixth-order coupling coefficient u_6 and the short-range lattice interaction coefficient K_2. In principle, it should at least be possible to extend the present RG flow calculations to the three-dimensional parameter space (u_0, r_0, K_2) by using the method of Ref. [10] to determine the coarse-grained short-range gradient coefficient $\tilde{K}_2$ for any given $K_2 \neq 0$. In particular, this extension should help to clarify the source of the mentioned discrepancies and also be useful to study the onset of crossover from long-range to the short-range critical behavior in the limit $\sigma \to 2-\eta_{\mathrm{SR}}$. However, such simulations and the fol-

TABLE I. Comparison of exponents y_τ, ω for various values of σ at $L=36$, $l=9$, $b=9/7$ calculated from simulation, perturbation theory, first- and second-order $\tilde{\epsilon}$-expansion, and an interpolation of the data of Ref. [14], respectively.

	y_τ					ω		
σ	Simulation	Perturbation	$O(\epsilon)$	$O(\epsilon^2)$	Ref. [14]	Simulation	Perturbation	$O(\epsilon)$
1.58	1.5290	1.53642	1.52667	1.52023	1.5198	0.1771	0.1789	0.16
1.60	1.5376	1.54666	1.53333	1.52347	1.523	0.1941	0.2400	0.2
1.64	1.5588	1.5751	1.5466	1.52808	1.52789	0.2889	0.32724	0.28
1.65	1.5595	1.57995	1.55951	1.52887	1.52886	0.3066	0.36680	0.3
1.70	1.5824	1.6165	1.56667	1.53088	1.53275	0.4066	0.523	0.4

lowing analysis of results would require extensive numerical work, which is why we must postpone them to the future. Nevertheless, we hope to have demonstrated that even though our method may not be the perfect tool for a high precision determination of critical exponents, it allows us to study the change in the topology of the RG flow of the long-range Ising model with varying $\tilde{\epsilon}$, something that—to our knowledge—has not been achieved with simulations before. Moreover, the numerical analysis of the flow pattern around the nontrivial fixed point sheds light on the role of the various approximations made in calculating universal quantities both qualitatively as well as quantitatively. We also expect our method to offer insight into the nature of the RG flow for other systems with long-range interactions. In particular, we plan to apply the method to the problem of fluctuating elastic membranes [18] and membranes with antiferroelectric water-filled nanopores [19].

ACKNOWLEDGMENTS

We would like to thank Professor H.W.J. Blöte, Professor C. Dellago, and Professor E. Luijten for helpful discussions and Professor C. Dellago for reading the paper.

[1] B. Delamotte and L. Canet, Condens. Matter Phys. **8**, 163 (2005).
[2] C. Bagnuls and C. Bervillier, Int. J. Mod. Phys. A **16**, 1825 (2001); Phys. Rep. **348**, 91 (2001).
[3] U. Schollwöck, Rev. Mod. Phys. **77**, 259 (2005); R. Bulla, T. A. Costi, and T. Pruschke, *ibid.* **80**, 395 (2008).
[4] A. N. Vasil'ev, *The Field Theoretic Renormalization Group in Critical Behavior Theory and Stochastic Dynamics* (Chapman and Hall, Boca Raton, 2004).
[5] K. G. Wilson and M. E. Fisher, Phys. Rev. Lett. **28**, 240 (1972).
[6] K. G. Wilson and J. B. Kogut, Phys. Lett., C **12**, 75 (1974).
[7] M. Kardar, *Statistical Physics of Fields* (Cambridge University Press, Cambridge, 2007); M. E. Peskin and D. V. Schroeder, *An Introduction to Quantum Field Theory* (Addison Wesley, Reading, 1997).
[8] As was first realized by Wilson and Kogut [6], a "hard cutoff" leads to certain pathologies and was consequently replaced by a "incomplete integration" procedure for a suitably chosen smooth weight function.
[9] J. Zinn-Justin, *Quantum Field Theory and Critical Phenomena* (Oxford Univ. Press, Oxford, 2002); D. Amit and V. Martin Mayor, *Field Theory, the Renormalization Group, and Critical Phenomena: Graphs to Computers*, 3rd ed. (World Scientific, Singapore, 2005); H. Kleinert and V. Schulte-Frohlinde, *Critical Properties of ϕ^4-Theories* (World Scientific, Singapore, 2001); G. Parisi, *Statistical Field Theory* (Perseus, New York, 1998).
[10] A. Tröster, Phys. Rev. B **76**, 012402 (2007); Comput. Phys. Commun. **179**, 30 (2008); Phys. Rev. Lett. **100**, 140602 (2008); A. Tröster and C. Dellago, Ferroelectrics **354**, 225 (2007).
[11] M. E. Fisher, S. K. Ma, and B. G. Nickel, Phys. Rev. Lett. **29**, 917 (1972).
[12] M. Suzuki, Y. Yamazaki, and G. Igarashi, Phys. Lett. **42A**, 313 (1972).
[13] J. Sak, Phys. Rev. B **8**, 281 (1973).
[14] E. Luijten, Ph.D. thesis, Delft University of Technology, 1997.
[15] E. Luijten and H. W. J. Blöte, Phys. Rev. B **56**, 8945 (1997); Phys. Rev. Lett. **89**, 025703 (2002).
[16] F. Wang and D. P. Landau, Phys. Rev. Lett. **86**, 2050 (2001); Phys. Rev. E **64**, 056101 (2001); F. Calvo, Mol. Phys. **100**, 3421 (2002); A. Tröster, C. Dellago, and W. Schranz, Phys. Rev. B **72**, 094103 (2005); A. Tröster and C. Dellago, Phys. Rev. E **71**, 066705 (2005).
[17] K. G. Wilson and M. E. Fisher, Phys. Rev. Lett. **28**, 548 (1972).
[18] *Statistical Mechanics of Membranes and Surfaces*, 2nd ed., edited by D. Nelson, T. Piran, and S. Weinberg (World Scientific, Singapore 1988).
[19] J. Köfinger, G. Hummer, and C. Dellago, Proc. Natl. Acad. Sci. U.S.A. **105**, 13218 (2008).